

# Photocatalytic Synthesis of Substituted Cyclic Carbonate Monomers for Ring-Opening Polymerization

Cristina Maquilón,<sup>a</sup> Francesco Della Monica,<sup>a</sup> Bart Limburg<sup>a\*</sup> and Arjan W. Kleij<sup>a,b\*</sup>

<sup>a</sup> Institute of Chemical Research of Catalonia (ICIQ), the Barcelona Institute of Science and Technology, Av. Països Catalans 16, 43007 - Tarragona, Spain. E-mail: [akleij@iciq.es](mailto:akleij@iciq.es), [blimburg@iciq.es](mailto:blimburg@iciq.es)

<sup>b</sup> Catalan Institute of Research and Advanced Studies (ICREA), Pg. Lluís Companys 23, 08010 Barcelona, Spain

Received: ###



Supporting information for this article is available on the WWW under <http://dx.doi.org/10.1002/adsc.2021###>

**Abstract.** An operationally mild, ruthenium-based photocatalytic protocol has been developed for the conversion of  $\gamma$ -mono- and  $\gamma,\gamma$ -disubstituted allyl carbonates in the presence of Umemoto's reagent to afford substituted six-membered cyclic carbonates. Variation and diversification of the carbonate ring substitution provides access to new

monomers useful in ring-opening polymerization leading to polycarbonates with potentially tailored properties, as illustrated by comparative experiments using monomers with different pi-stacking capabilities.

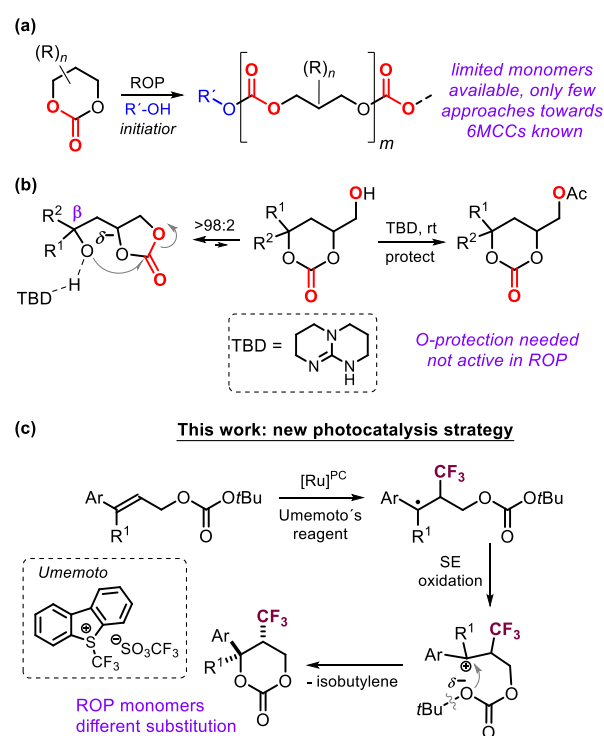
**Keywords:** Cyclic carbonates; Photocatalysis; Ring-opening polymerization; Ruthenium; Trifluoromethyl

## Introduction

Aliphatic polycarbonates have received significant attention due to their favorable biodegradation and biocompatibility features enabling these polymers as useful ingredients of materials for biomedical applications and advanced materials.<sup>[1]</sup> The synthesis of polycarbonates can be achieved via the ring-opening copolymerization (ROCOP) of epoxides and CO<sub>2</sub>, though over the years relatively few monomer combinations have shown promise towards selective formation of fully alternating polycarbonates with tunable properties.<sup>[2]</sup> This lack of diversity provides impetus for new monomer engineering as to design novel types of functional polycarbonates whose properties can be more precisely tailored.

The ring-opening polymerization (ROP) of cyclic carbonates represents another route towards the synthesis of polycarbonate macromolecules.<sup>[3]</sup> Whereas the synthesis of five-membered cyclic carbonates (5MCCs) is well-established,<sup>[4]</sup> there is comparatively low ROP potential for these types of heterocycles, and there exist only a few known examples that exploit the reactivity of *trans*-fused, strained polycyclic carbonate structures.<sup>[5]</sup> Unlike their five-membered analogues, the ROP of larger-ring carbonates has been reported as a viable strategy towards the preparation of polycarbonates.<sup>[6]</sup> In particular, the ROP of six-membered carbonates has been most frequently studied building on a more diverse set of available monomers, thereby creating polycarbonate variability (Scheme 1a).<sup>[7]</sup> However, the synthesis of six-membered cyclic carbonates (6MCCs) can be tedious and only a handful of effective methods

have been reported so far.<sup>[8]</sup> Among the general approaches, the use of catalytic oxetane/CO<sub>2</sub> coupling reactions<sup>[9]</sup> and the stoichiometric conversion of diol reagents<sup>[10]</sup> are noteworthy.



**Scheme 1.** (a) ROP of 6MCCs leading to aliphatic polycarbonates. (b) Previous approach to 6MCCs using 5MCC as precursors. (c) Current photocatalytic strategy to forge novel types of 6MCCs. PC stands for photocatalyst.

In a more recent approach, our group demonstrated that tri-substituted 6MCCs can be obtained from 5MCCs that comprise of  $\beta$ -positioned (*exo*-cyclic) alcohol groups that upon activation by base allow for an unusual isomerization process (Scheme 1b).<sup>[11]</sup> In this latter approach, it was necessary to protect the alcohol group of the 6MCC product to prevent back-equilibration to the thermodynamically more stable 5MCC. Preliminary ROP experiments with this type of 6MCC, however, were unsuccessful and inspired us to devise new synthetic methods to create different types of 6MCC monomers. In this regard, the use of photoredox catalysis was considered as such an approach was previously successfully applied to prepare 5MCCs<sup>[12a]</sup> and related oxazolidinones.<sup>[12]</sup> As far as we are aware, no efforts have been described to create larger-ring carbonates under photocatalytic conditions.

Our envisioned approach is based on the use of readily available, *O*-Boc-protected  $\gamma$ -substituted allylic alcohols (Scheme 1c). Under suitable photocatalytic conditions, radical addition to the allylic precursor should be feasible giving a stabilized benzylic radical. Subsequent single-electron oxidation produces a benzylic cation that can be intercepted intramolecularly by the OBoc fragment to give the 6MCC target, under expulsion of isobutylene. Here we present the results of this photocatalysis strategy towards 6MCCs, the evaluation of their ROP potential and the influence of the carbonate ring substitution.

## Results and Discussion

We first selected Boc-protected cinnamyl alcohol as a benchmark substrate for our screening studies while using a Umemoto reagent as a source of CF<sub>3</sub> radicals<sup>[13]</sup> generated under blue LED irradiation using transition metal photoredox catalysts (PCs, Table 1). In the presence of NaHCO<sub>3</sub> (entry 1), good conversion of **1a** was achieved after 30 min producing **2a** in 32% NMR yield. A longer reaction time (entry 2, 3 h) did not improve this result, and we found that the addition of base (entry 3, 27% of **2a** formed) is not necessary.

We thus continued without this additive and investigated the influence of the concentration (entries 4–6), solvent (entries 7–10), the nature of the PC (entries 11–14), the excess of Umemoto reagent (entry 15) and the temperature / light intensity (entry 16 and 17). A concentration of 18 mM proved to be optimal producing **2a** in 54% yield, whereas changing the solvent did not improve the process outcome. Variation of the PC from **A** to **B–E** also did not lead to improved efficiency and increasing the amount of Umemoto's reagent from 1.1 to 1.5 equiv (entry 15) showed virtually no change in the yield of **2a**. While decreasing the light intensity led to a drop in chemoselectivity (entry 16), some improvement was noted when increasing the light intensity while carrying out the catalytic protocol at 0 °C giving **2a** in 66% NMR and 62% isolated yield (entry 17).

A number of control reactions were performed (Table 2) to scrutinize the role of the reactants and catalyst. In the dark (entry 1), the chemo-selectivity towards **2a** drops significantly.

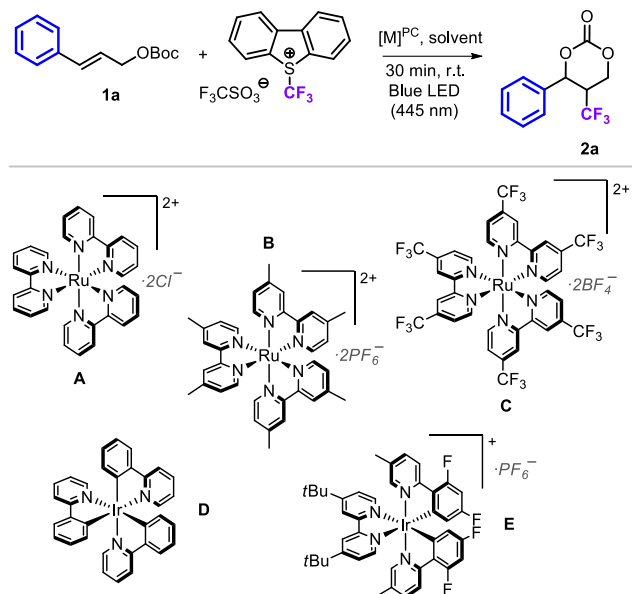


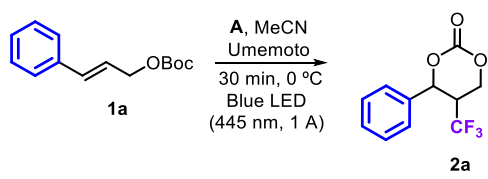
**Table 1.** Photocatalytic conversion of *O*-Boc protected cinnamyl alcohol **1a** into 6MCC **2a** under various conditions.<sup>[a]</sup>

| Entry              | Solvent / PC       | Conc. [mM] | Conv. <b>1a</b> [%] <sup>[b]</sup> | Yield <b>2a</b> [%] <sup>[c]</sup> |
|--------------------|--------------------|------------|------------------------------------|------------------------------------|
| 1 <sup>[d]</sup>   | MeCN / <b>A</b>    | 180        | 91                                 | 32                                 |
| 2 <sup>[d,e]</sup> | MeCN / <b>A</b>    | 180        | 98                                 | 23                                 |
| 3                  | MeCN / <b>A</b>    | 180        | >99                                | 27                                 |
| 4                  | MeCN / <b>A</b>    | 9          | >99                                | 37                                 |
| 5                  | MeCN / <b>A</b>    | 18         | >99                                | 54                                 |
| 6                  | MeCN / <b>A</b>    | 36         | >99                                | 46                                 |
| 7                  | DCM / <b>A</b>     | 18         | >99                                | 13                                 |
| 8                  | DMF / <b>A</b>     | 18         | 45                                 | 5                                  |
| 9                  | DMSO / <b>A</b>    | 18         | 90                                 | 7                                  |
| 10                 | Acetone / <b>A</b> | 18         | >99                                | 13                                 |
| 11                 | MeCN / <b>B</b>    | 18         | >99                                | 32                                 |
| 12                 | MeCN / <b>C</b>    | 18         | 0 <sup>[f]</sup>                   | 0                                  |
| 13                 | MeCN / <b>D</b>    | 18         | 91                                 | 13                                 |
| 14                 | MeCN / <b>E</b>    | 18         | >99                                | 21                                 |
| 15 <sup>[g]</sup>  | MeCN / <b>A</b>    | 18         | >99                                | 55                                 |
| 16 <sup>[h]</sup>  | MeCN / <b>A</b>    | 18         | >99%                               | 39                                 |
| 17 <sup>[i]</sup>  | MeCN / <b>A</b>    | 18         | >99                                | 66 (62) <sup>[j]</sup>             |

[a] **1a** (0.18 mmol for entries 1-3 and 6; 0.045 mmol for entry 4; 0.09 mmol for entries 5 + 7-17), Umemoto reagent (1.1 equiv), RuCl<sub>2</sub>(bpy)<sub>3</sub>·6H<sub>2</sub>O (**A**, 1.0 mol%), solvent (concentration stated), 30 min, rt, blue LED irradiation ( $\lambda_{em}$  = 445 nm, 700 mA, corresponding to 1.2  $\mu$ einstein/s. [b] Determined by <sup>1</sup>H NMR (CDCl<sub>3</sub>). [c] As for [b] using mesitylene as internal standard. [d] With NaHCO<sub>3</sub> as additive (3 equiv.). [e] Reaction time was 3 h. [f] Using **C** as PC, no conversion of **1a**/Umemoto reagent observed. [g] Using 1.5 equiv Umemoto reagent. [h] LED current was 200 mA, corresponding to a photon flux of 0.4  $\mu$ einstein/s. [i] LED current was 1000 mA, corresponding to a photon flux of 1.6  $\mu$ einstein/s, T = 0 °C. [j] In brackets, the isolated yield of **1a**.

The presence of light and PC **A** (entry 1 & 2) are a requisite for product formation. Dioxygen proved to affect the reaction only marginally (entry 3) and the yield did not increase if the purification was omitted, indicating no material is lost in the workup (entry 4). The addition of water (entry 5) lowered the yield of **2a** to 46%. In the absence of starting material, Umemoto's reagent was fully converted to dibenzothiophene, indicating that photoexcitation of the PC leads to formation of CF<sub>3</sub> radicals also in the absence of **1a**. The liberation of dibenzothiophene during the conversion of Umemoto's reagent and its potential effect on the catalytic efficiency was also probed but no significant decrease in product yield was noted (entry 7). Finally, the addition of TEMPO (entry 8) shut down the reaction completely in line with the envisioned intermediacy of benzylic and CF<sub>3</sub> radicals (Scheme 1c). Substrates lacking benzylic stabilization of the radical intermediate, such as Boc-protected prenyl led to complicated product mixtures. Other protective groups such as methoxycarbonyl or ethoxycarbonyl produced **2a** in much lower yield (entries 9 and 10), indicating that the acid-labile Boc-group is deprotected by the intermediate acidic benzylic cation. Fluorocarbon radical precursors such as Togni reagent II, TMSCF<sub>3</sub> or perfluorohexyl iodide were unproductive, likely due to their inability to quench the excited state.

**Table 2.** Control experiments carried out under the optimized screening conditions.<sup>[a]</sup>

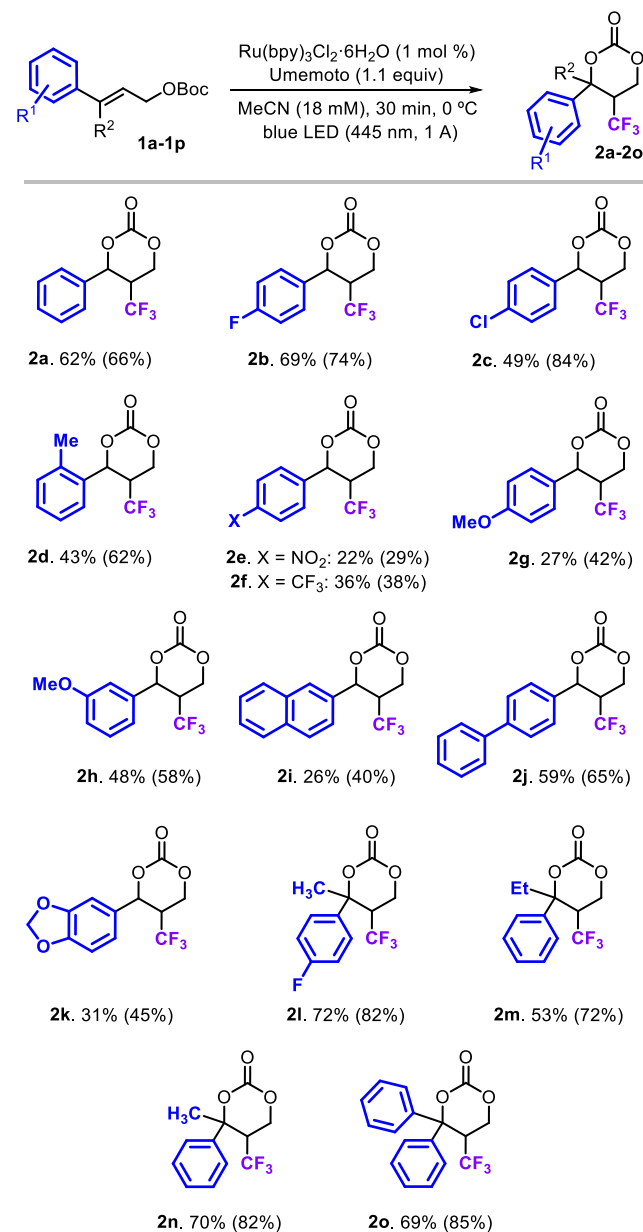


| Entry            | Deviation                         | Yield <b>2a</b> [%] <sup>[b]</sup> |
|------------------|-----------------------------------|------------------------------------|
| 1                | In the dark                       | 4                                  |
| 2                | No PC ( <b>A</b> ) added          | 3                                  |
| 3                | No degassing                      | 52                                 |
| 4                | No extraction                     | 50                                 |
| 5                | Added 10 $\mu$ L H <sub>2</sub> O | 46                                 |
| 6                | No <b>1a</b> added                | 0 <sup>[c]</sup>                   |
| 7                | Dibenzothiophene (1 equiv) added  | 60                                 |
| 8 <sup>[d]</sup> | TEMPO (2 equiv) added             | 0                                  |
| 9                | Methoxycarbonyl instead of boc    | 13                                 |
| 10               | Ethoxycarbonyl instead of boc     | 8                                  |

[a] See entry 17, Table 1. [b] Determined by <sup>1</sup>H NMR (CDCl<sub>3</sub>) using mesitylene as internal standard. [c] Full conversion of Umemoto's reagent was observed by <sup>1</sup>H NMR. [d] TEMPO-CF<sub>3</sub> adduct (12%) observed by <sup>19</sup>F NMR analysis.

The maximum (NMR) yield for **2a** was thus 66%, and a full kinetic profile (with a total time frame of 5 min; see the Supporting Information, SI, for details)

for the transformation was established. Interestingly, in the beginning of the reaction (first 20 sec), both the conversion of **1a** and the formation of **2a** develop with a fully accounted mass balance, though shortly hereafter the amount of byproduct quickly increases to about 31% after 5 min. <sup>19</sup>F NMR analysis of the crude product at this stage illustrated a variety of products, which we ascribe to the formation of trifluoromethylated (oligomeric) styrenes.



**Scheme 3.** Product scope for the photocatalytic formation of 6MCCs providing the products **2a-2o**. Yields are of the isolated, column-purified products with in parentheses the NMR yield using 1,3,5-tris(trifluoromethyl)benzene as internal standard.

The reason for this change in chemoselectivity with time can be explained by the instability of photocatalyst **A** under turnover conditions. As shown in Figure S1 (SI), the UV-vis spectrum shows that the

characteristic band of **A** changes during the reaction, indicating its decomposition. It is likely that CF<sub>3</sub> radicals react with the bipyridine ligands, altering the photophysical and photochemical properties of the photocatalyst rendering it unproductive for the reaction (*cf.* efficiency of photocatalyst **A** versus **C**). Though a lower yield for **2a** is the consequence of competitive side-reactions, the targeted product can be easily isolated by column purification.<sup>[14]</sup> From the kinetic data, we further infer that the initial quantum yield of the reaction is 158%, indicating a radical propagation mechanism (see Figure S3, SI). Stern-Volmer analysis (Figure S2, SI) shows that the reaction commences by oxidative quenching to form [Ru(bpy)<sub>3</sub>]<sup>3+</sup> and a CF<sub>3</sub> radical which adds to the double bond. The resulting benzylic radical is then oxidized by Umemoto's reagent (radical propagation) or by [Ru(bpy)<sub>3</sub>]<sup>3+</sup> (termination) following ring-closure to yield **2a** (Scheme 1c and Figure S3).

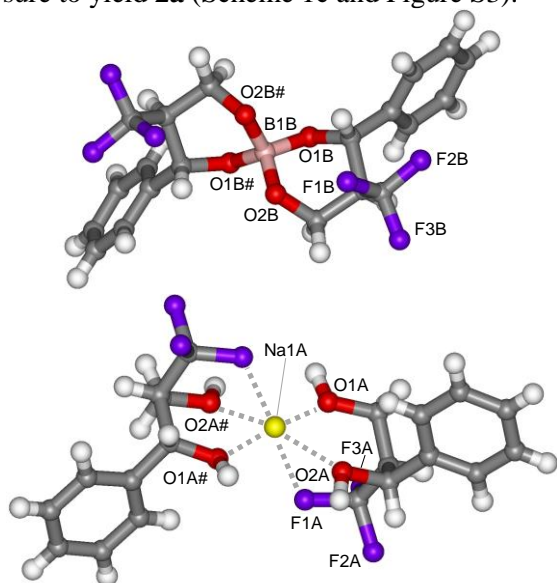


**Figure 1.** Molecular structure determined for sodium borate derived from **2a**. Top: borate anion based on two decarbonylated molecules of **2a**. Below: sodium cation stabilized by two 1,3-diols derived from **2a** showing weak F...Na cation interactions. Selected bond lengths (Å) and angles (°) with esd's in parentheses: B1B–O1B = B1B–O1B# = 1.465(3), B1B–O2B = B1B–O2B# = 1.474(3), Na1A–O1A = 2.2119(19), Na1A–O1A# = 2.3016(19), Na1A–O2A = 2.227(2), Na1A–O2A# = 2.255(2), Na1A–F1A = 2.5089(18); O1B–B1B–O1B# = 107.2(3), O2B–B1B–O2B# = 106.2(3), O1B–B1B–O2B = 108.73(10), O1B–B1B–O2B# = 113.03(9), O1A–Na1A–O1A# = 102.93(10), O2A–Na1A–O2A# = 94.05(11), O1A–Na1A–O2A = 81.27(6), O1A–Na1A–O2A# = 171.00(8).

The optimized reaction conditions (Table 1, entry 17) were then applied to the synthesis of a wider scope of 6MCCs (Scheme 3, **2a-2o**). Various mono- $\gamma$ -aryl allylic carbonates could be converted into their respective 6MCCs in moderate to appreciably high NMR yields of up to 84% (**2a-2k**), with lower yields

observed for substrates carrying electron-withdrawing substituents (**2e** and **2f**) and those equipped with a 4-methoxy-aryl (**2g**), 2-naphthyl (**2i**) or a heterobicycle (**2k**). The exact influence of each aryl substitution on the stability and reactivity of the benzylic radical/cation intermediates depicted in Scheme 1c is not entirely clear. However, we further noted that a di- $\gamma$ -substitution in the allylic carbonate (*cf.*, syntheses of **2l-2o**) was beneficial providing among the highest 6MCC NMR (up to 85%) and isolated yields (up to 72%) suggesting a better control over the reactivity of the aforementioned intermediates. The larger discrepancy between some of the NMR and isolated yields is explained by the fact that some of these 6MCCs proved to be rather sensitive during column purification, yielding substantial amounts of 1,3-diol byproduct by hydrolysis provoked by the acidic sites of the SiO<sub>2</sub> stationary phase. Therefore, all 6MCC products were isolated as quickly as possible, minimizing the contact-time with the SiO<sub>2</sub>-based column material.

All 6MCC products were fully characterized by spectroscopic and spectrometric analyses (see the SI). Further to this, crystalline material was obtained from two different product samples. Though **2a** was initially isolated as a viscous oil, a crystallization attempt that covered a period of several months produced a crystalline compound that was analyzed by X-ray crystallography (Figure 1). Surprisingly, the structure of an unexpected sodium borate ion pair was revealed that incorporates in total four “decarbonylated” molecules of **2a**. Due to this serendipitous result,<sup>[15]</sup> an *anti*-positioning between the CF<sub>3</sub> and aryl group could be determined suggesting a preferred mutual orientation in the ring-closure step leading to 6MCC **2a** (Scheme 1c).

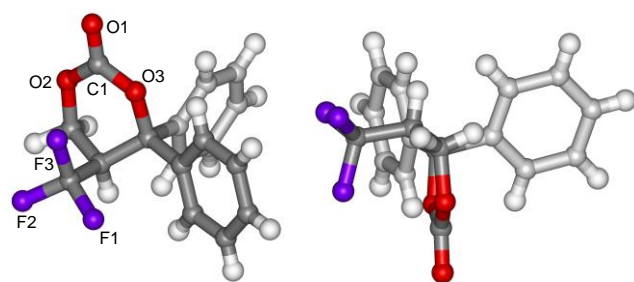


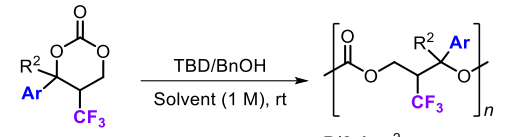
**Figure 2.** Molecular structure determined for 6MCC **2o**. Left: front view. Right: side view. Selected bond lengths (Å) and angles (°) with esd's in parentheses: O1–C1 = 1.2048(10), O2–C1 = 1.3388(9), O3–C1 = 1.3317(10); O2–C1–O3 = 119.95(7), O1–C1–O2 = 119.48(7), O2–C1–O3 = 119.95(7).

The molecular connectivity of carbonate product **2o** was confirmed by X-ray analysis (Figure 2). The structure illustrates that the three carbonate ring substituents increase the steric requirements around the carbonate unit, which may affect its reactivity in ROP studies (*vide infra*).



We investigated the possibility to use cyclic carbonates **2** as monomers in ROP reactions (Table 3). Previous investigations showed that 1,5,7-triazabicyclo[4.4.0]dec-5-ene (TBD) is an efficient organocatalyst for the ROP of 6MCCs.<sup>[16]</sup> Thus, the TBD-catalyzed ROP of **2a**, using BnOH as initiator, was first investigated to examine the potential of the new 6MCCs (Scheme 3) in the preparation of polycarbonates. The reaction was first conducted in DCM under similar conditions used for other 6MCCs.<sup>[17,18]</sup> Low conversion of **2a** was observed after 20 h, while the conversion level increased to 34% in toluene (entries 1 and 2). An increase in the catalyst loading to 2 mol% resulted in higher conversion of **2a** (entry 3). Attempts to obtain full conversion by increasing the reaction temperature up to 100 °C led to similar monomer conversion though lower polycarbonate selectivity (45%) due to hydrolysis towards the 1,3-diol (entry 4). Instead, higher monomer conversion could be obtained prolonging the reaction time, maintaining a polycarbonate selectivity of >99% and affording **P(2a)** with a  $M_n$  of 5.2 kg·mol<sup>-1</sup> (entry 5).

**Table 3.** Ring-opening polymerization of 6MCCs **2a**, **2i** and **2j** promoted by TBD/BnOH.<sup>[a]</sup>



**P(2a):** R<sup>2</sup> = H, Ar = Ph  
**P(2i):** R<sup>2</sup> = H, Ar = 2-naphthyl  
**P(2j):** R<sup>2</sup> = H, Ar = 4-biphenyl

| Entry            | <b>2</b>  | TBD<br>[mol%] | Time<br>[h] | Conv.<br>[%] <sup>[b]</sup> | $M_n$ <sup>[c]</sup> | $\bar{D}$ <sup>[c]</sup> |
|------------------|-----------|---------------|-------------|-----------------------------|----------------------|--------------------------|
| 1 <sup>[d]</sup> | <b>2a</b> | 1             | 20          | 17                          | –                    | –                        |
| 2                | <b>2a</b> | 1             | 20          | 34                          | –                    | –                        |
| 3                | <b>2a</b> | 2             | 20          | 62                          | 3.1                  | 1.39                     |
| 4 <sup>[e]</sup> | <b>2a</b> | 2             | 20          | 58                          | –                    | –                        |
| 5 <sup>[f]</sup> | <b>2a</b> | 1             | 60          | 78                          | 5.2                  | 1.42                     |
| 6 <sup>[g]</sup> | <b>2i</b> | 1             | 76          | 83                          | 5.0                  | 1.23                     |
| 7 <sup>[h]</sup> | <b>2j</b> | 1             | 66          | 59                          | 2.6                  | 1.41                     |

[a] monomer **2** ( $8.1 \cdot 10^{-5}$  mol), TBD/BnOH = 1/1, toluene (82  $\mu$ L; 1.0 M), rt. [b] Determined by <sup>1</sup>H NMR (CDCl<sub>3</sub>). [c] Determined by GPC in THF calibrated with polystyrene standards.  $M_n$  values in kg·mol<sup>-1</sup>. [d] The solvent was dichloromethane. [e] Reaction temperature was 100 °C. [f] Amount of **2a** was 100 mg ( $4.1 \cdot 10^{-4}$  mol). [g] Amount of **2i** was  $1.1 \cdot 10^{-4}$  mol. [h] Amount of **2j** was  $2.6 \cdot 10^{-4}$  mol.

Following these results obtained with monomer **2a**, cyclic carbonates with different aryl substitutions were tested under the same conditions as monomer **2a** (entry 5). Naphthyl (**2i**) and biphenyl (**2j**) substituted 6MCCs were converted with moderate to high conversion levels providing oligo/polycarbonates **P(2i)** and **P(2j)** with molecular weight distributions ( $\bar{D}$ ) comparable with that of **P(2a)** (entries 6 and 7), but the  $M_n$  value measured for **P(2j)** was lower (2.6 kg·mol<sup>-1</sup>). Unfortunately, ROP attempts using either carbonates **2n** or **2o** containing quaternary carbon centers only led

to the hydrolysis products. The steric impediment around the carbonate carbon center in **2o** revealed by X-ray analysis is in line with this observation and likely the ROP process is significantly inhibited

The new **P(2a)**, **P(2i)** and **P(2j)** were characterized by NMR confirming the formation of the desired polycarbonates (see the SI for details). Diagnostic benzylic signals could be detected between 5.0 and 5.1 ppm in the <sup>1</sup>H NMR spectra, which can be assigned to the benzyl alcohol initiator.

Decomposition temperatures ( $T_{5\%}$ ) were determined by thermogravimetric analyses (TGA) under nitrogen recording values of 182, 194 and 186 °C for **P(2a)**, **P(2i)** and **P(2j)**, respectively (see the SI). Despite the fact that these values are not very high, they are close to the decomposition temperature of poly(propylene carbonate) having similar (low) molecular weight.<sup>[19]</sup>

Glass transition temperatures ( $T_g$ 's) of **P(2a)**, **P(2i)** and **P(2j)** were determined by differential scanning calorimetry (DSC) providing values of 37, 65 and 56 °C, respectively (see the SI). Comparison of these values with the  $T_g$  (–15 °C)<sup>[20]</sup> of the simplest unsubstituted poly(trimethylene carbonate), PTMC, demonstrates that by introduction of substituents in the main chain of the oligo/polycarbonate reduces its flexibility resulting in substantially higher  $T_g$  values.

## Conclusion

We here present a synthetic route for the formation of substituted 6MCCs through a photocatalytic conversion of readily available  $\gamma$ -substituted allylic carbonates. A reasonable scope of 6MCCs was produced with different degrees of carbonate ring substitution. Additional ROP studies have established that these 6MCCs are indeed monomers for new types of polycarbonates with glass transitions that are at markedly higher temperatures than measured for the parent PTMC. The substitution degree and identity of the ring-substituents are likely key elements to develop modular type polycarbonates from larger ring cyclic carbonates with improved thermal properties.

## Experimental Section

### Typical Synthesis of the 6MCC Products

In a flat-bottom Schlenk, 5-(trifluoromethyl)dibenzo-thiophenium trifluoromethanesulfonate (Umemoto's reagent, 99  $\mu$ mol, 1.1 equiv) and Ru(bpy)<sub>3</sub>Cl<sub>2</sub>·6H<sub>2</sub>O (0.90  $\mu$ mol, 1.0 mol%) were introduced, after which carefully three cycles of vacuum/N<sub>2</sub> filling were carried out. Then, dry CH<sub>3</sub>CN and finally *tert*-butyl cinnamyl carbonate (90  $\mu$ mol, 21.1 mg) were added. The Schlenk reactor was allowed to reach the desired temperature in the photoreactor until a homogeneous mixture was obtained and then the reaction mixture was irradiated during 30 min. Once completed, the reaction mixture was diluted by CH<sub>2</sub>Cl<sub>2</sub> and water was added. The aqueous phase was extracted with CH<sub>2</sub>Cl<sub>2</sub>, the organic layers combined and dried over Na<sub>2</sub>SO<sub>4</sub> and concentrated. The crude product was further purified via column chromatography (hexane:EtOAc, gradient from 4:1 to 2:1) obtaining **2a** as a colorless oil (13.7 mg, 62% yield).

For a collection of the characterization data of all compounds and the reactor details, see the SI.

### Typical ROP of selected 6MCCs

In a glovebox, monomer **2a** (20 mg, 81  $\mu\text{mol}$ ) was introduced into a vial equipped with a magnetic stirrer. Then, benzyl alcohol (27  $\mu\text{L}$  from a 59.2 mM solution in toluene, 1.62  $\mu\text{mol}$ , 2.0 mol%) and TBD (55  $\mu\text{L}$  of a 29.5 mM solution in toluene, 1.62  $\mu\text{mol}$ , 2 mol%) were added in this sequence. Out of the glovebox, the vial was sealed with electric insulator tape. After stirring for 20 h, the reaction mixture was quenched with benzoic acid (30  $\mu\text{L}$  of a 83.5 mM solution in toluene, 1.22  $\mu\text{mol}$ ) and a sample was analyzed by NMR to determine the monomer conversion. The polymer product was collected by precipitation from hexane and filtration. Conversion of **2a** under these conditions was 62%.  $M_n$  (GPC) = 3.1 kDa. See the SI for more details.

### X-ray Molecular Determinations

The measured crystals were stable under atmospheric conditions; nevertheless, they were treated under inert conditions immersed in perfluoro-polyether as protecting oil for manipulation. Data Collection: measurements were made on a Bruker-Nonius diffractometer equipped with an APPEX II 4 K CCD area detector, a FR591 rotating anode with Mo  $K\alpha$  radiation, Montel mirrors and a Kryoflex low temperature device ( $T = -173$  °C). Full-sphere data collection was used with  $\omega$  and  $\phi$  scans. Programs used: data collection Apex2V2011.3 (Bruker-Nonius 2008), data reduction SAINT+Version 7.60A (Bruker AXS 2008) and absorption correction SADABS V. 2008-1 (2008). Structure solution: SHELXTLVersion 6.10 (Sheldrick, 2000) was used.<sup>[21]</sup> Structure refinement: SHELXTL-97-UNIX VERSION.

Crystal data for the sodium borate derived from **2a**:  $\text{C}_{40}\text{H}_{40}\text{BF}_{12}\text{NaO}_8$ ,  $M_r = 910.52$ , monoclinic,  $I2/a$ ,  $a = 21.8987(6)$  Å,  $b = 9.4206(2)$  Å,  $c = 19.8167(6)$  Å,  $\alpha = 90^\circ$ ,  $\beta = 90.507(3)^\circ$ ,  $\gamma = 90^\circ$ ,  $V = 4088.00(19)$  Å<sup>3</sup>,  $Z = 4$ ,  $\rho = 1.479$  mg·M<sup>-3</sup>,  $\mu = 0.145$  mm<sup>-1</sup>,  $\lambda = 0.71073$  Å,  $T = 100(2)$  K,  $F(000) = 1872$ , crystal size =  $0.20 \times 0.20 \times 0.03$  mm,  $\theta(\text{min}) = 2.055^\circ$ ,  $\theta(\text{max}) = 27.133^\circ$ , 16469 reflections collected, 3888 reflections unique ( $R_{\text{int}} = 0.0371$ ),  $\text{GoF} = 1.028$ ,  $R_1 = 0.0484$  and  $wR_2 = 0.1217$  [ $I > 2\sigma(I)$ ],  $R_1 = 0.0969$  and  $wR_2 = 0.1413$  (all indices), min/max residual density =  $-0.301/0.465$  [e·Å<sup>-3</sup>]. Completeness to  $\theta(27.133^\circ) = 86.0\%$ . CCDC number 2074284.

Crystal data for 6MCC **2o**:  $\text{C}_{17}\text{H}_{13}\text{F}_3\text{O}_3$ ,  $M_r = 322.27$ , monoclinic,  $P2_1/n$ ,  $a = 8.32649(10)$  Å,  $b = 16.25304(18)$  Å,  $c = 10.67489(14)$  Å,  $\alpha = 90^\circ$ ,  $\beta = 92.3904(12)^\circ$ ,  $\gamma = 90^\circ$ ,  $V = 1443.38(3)$  Å<sup>3</sup>,  $Z = 4$ ,  $\rho = 1.483$  mg·M<sup>-3</sup>,  $\mu = 0.126$  mm<sup>-1</sup>,  $\lambda = 0.71073$  Å,  $T = 100(2)$  K,  $F(000) = 664$ , crystal size =  $0.25 \times 0.20 \times 0.10$  mm,  $\theta(\text{min}) = 2.506^\circ$ ,  $\theta(\text{max}) = 34.42^\circ$ , 29596 reflections collected, 5868 reflections unique ( $R_{\text{int}} = 0.0243$ ),  $\text{GoF} = 1.049$ ,  $R_1 = 0.0378$  and  $wR_2 = 0.1078$  [ $I > 2\sigma(I)$ ],  $R_1 = 0.0436$  and  $wR_2 = 0.1111$  (all indices), min/max residual density =  $-0.267/0.525$  [e·Å<sup>-3</sup>]. Completeness to  $\theta(34.42^\circ) = 96.8\%$ . CCDC number 2074285.

### Acknowledgements

We thank the Cerca program/Generalitat de Catalunya, ICREA, MINECO (CTQ2017-88920-P and FPI fellowship to CM), AGAUR (2017-SGR-232) and the Ministerio de Ciencia e Innovación (Severo Ochoa Excellence Accreditation 2020–2023 CEX2019-000925-S and PID2020-112684GB-I00) for support. BL and FDM thank the European Community for Marie Curie individual fellowships (PHOTOCARBOX-889754 and SUPREME-840557). Dr. E.C.

Escudero-Adán and Dr. M. Martínez Belmonte are acknowledged for the X-ray crystallographic studies.

## References

- [1] a) J. Xu, E. Feng, J. Song, *J. Appl. Polym. Sci.* **2014**, *131*, 39822; b) J. Feng, R.-X. Zhuo, X.-Z. Zhang, *Polym. Sci.* **2012**, *37*, 211–236; c) Y. Daia, X. Zhang, *Polym. Chem.* **2017**, *8*, 7429–7437; d) W. Yu, E. Maynard, V. Chiaradia, M. C. Arno, A. P. Dove, *Chem. Rev.* **2021**, DOI: 10.1021/acs.chemrev.0c00883; e) A. Domiński, T. Konieczny, K. Duale, M. Krawczyk, G. Pastuch-Gawolek, P. Kurcok, *Polymers* **2020**, *12*, 2890; f) W. Chen, F. Meng, R. Cheng, C. Deng, J. Feijen, Z. Zhong, *J. Controlled Release* **2014**, *190*, 398–414; g) F. Suriano, R. Pratt, J. P. K. Tan, N. Wiradharma, A. Nelson, Y.-Y. Yang, P. Dubois, J. L. Hedrick, *Biomaterials* **2010**, *31*, 2637–2645; h) K. Fukushima, *Biomater. Sci.* **2016**, *4*, 9–24; i) B. Grignard, S. Gennen, C. Jérôme, A. W. Kleij, C. Detrembleur, *Chem. Soc. Rev.* **2019**, *48*, 4466–4514.
- [2] For selected examples: a) G.-P. Wu, S.-H. Wei, W.-M. Ren, X.-B. Lu, B. Li, Y.-P. Zu, D. J. Darensbourg, *Energy & Environmental Sci.* **2011**, *4*, 5084–5092; b) G.-P. Wu, P.-X. Xu, X.-B. Lu, Y.-P. Zu, S.-H. Wei, W.-M. Ren, D. J. Darensbourg, *Macromolecules* **2013**, *46*, 2128–2133; c) D. J. Darensbourg, S. J. Wilson, *J. Am. Chem. Soc.* **2011**, *133*, 18610–18613; d) D. J. Darensbourg, W.-C. Chung, S. J. Wilson, *ACS Catal.* **2013**, *3*, 3050–3057; e) O. Hauenstein, S. Agarwal, A. Greiner, *Nat. Commun.* **2016**, *7*, 11862; f) C. Li, R. J. Sablong, C. E. Koning, *Angew. Chem. Int. Ed.* **2016**, *55*, 11572–11576; g) N. Kindermann, À. Cristòfol, A. W. Kleij, *ACS Catal.* **2017**, *7*, 3860–3863.
- [3] S. Tempelaar, L. Mespouille, O. Coulembier, P. Dubois, A. P. Dove, *Chem. Soc. Rev.* **2013**, *42*, 1312–1336; b) G. Rokicki, *Prog. Polym. Sci.* **2000**, *25*, 259–342; c) S. M. Guillaume, L. Mespouille, *J. Appl. Polym. Sci.* **2014**, *131*, 40081; d) N. Ajellal, J.-F. Carpentier, C. Guillaume, S. M. Guillaume, M. Helou, V. Poirier, Y. Sarazin, A. Trifonov, *Dalton Trans.* **2010**, *39*, 8363–8376.
- [4] For some reviews: a) R. Rajjak Shaikh, S. Pornpraprom, V. D'Elia, *ACS Catal.* **2018**, *8*, 419–450; b) J. W. Comerford, I. D. V. Ingram, M. North, X. Wu, *Green Chem.* **2015**, *17*, 1966–1987; c) V. Aomchad, À. Cristòfol, F. Della Monica, B. Limburg, V. D'Elia, A. W. Kleij, *Green Chem.* **2021**, *23*, 1077–1113; d) F. Della Monica, A. W. Kleij, *Catal. Sci. Technol.* **2020**, *10*, 3483–3501.
- [5] a) M. Azechi, K. Matsumoto, T. Endo, *J. Polym. Sci., Part A: Polym. Chem.* **2013**, *51*, 1651–1655; b) K. Tezuka, K. Koda, H. Katagiri, O. Haba, *Polym. Bull.* **2015**, *72*, 615–626.
- [6] Selected examples of ROP of larger-ring carbonates: a) S. Venkataraman, V. W. L. Ng, D. J. Coady, H. W. Horn, G. O. Jones, T. S. Fung, H. Sardon, R. M. Waymouth, J. L. Hedrick, Y. Y. Yang, *J. Am. Chem. Soc.* **2015**, *137*, 13851–13860; b) T. M. McGuire, C.

- Pérale, R. Castaing, G. I. Kociok-Köhn, A. Buchard, *J. Am. Chem. Soc.* **2019**, *141*, 13301-13305; c) Y. Song, X. Yang, Y. Shen, M. Dong, Y.-N. Lin, M. B. Hall, K. L. Wooley, *J. Am. Chem. Soc.* **2020**, *142*, 16974-16981; d) P. Brignou, M. Priebe Gil, O. Casagrande, J.-F. Carpentier, S. M. Guillaume, *Macromolecules* **2010**, *43*, 19, 8007-8017.
- [7] a) E. M. López-Vidal, G. L. Gregory, G. Kociok-Köhn, A. Buchard, *Polym. Chem.* **2018**, *9*, 1577-1582; b) G. L. Gregory, G. Kociok-Köhn, A. Buchard, *Polym. Chem.* **2017**, *8*, 2093-2104; c) G. L. Gregory, L. M. Jenisch, B. Charles, G. Kociok-Köhn, A. Buchard, *Macromolecules* **2016**, *49*, 7165-7169; d) G. A. Bhat, M. Luo, D. J. Darensbourg, *Green Chem.* **2020**, *22*, 7707-7724; e) D. J. Darensbourg, A. I. Moncada, S.-H. Wei, *Macromolecules* **2011**, *44*, 2568-2576; f) M. Helou, O. Miserque, J.-M. Brusson, J.-F. Carpentier, S. M. Guillaume, *Chem. Eur. J.* **2010**, *16*, 13805-13813; g) Y. Shen, X. Chen, R. A. Gross, *Macromolecules* **1999**, *32*, 2799-2802.
- [8] a) B. A. Vara, T. J. Struble, W. Wang, M. C. Dobish, J. N. Johnston, *J. Am. Chem. Soc.* **2015**, *137*, 7302-7305; b) S. Minakata, I. Sasaki, T. Ide, *Angew. Chem. Int. Ed.* **2010**, *49*, 1309-1311.
- [9] a) B. R. Buckley, A. P. Patel, K. G. Upul Wijayantha, *Eur. J. Org. Chem.* **2014**, 474-478; b) C. J. Whiteoak, E. Martin, M. Martínez Belmonte, J. Benet-Buchholz, A.W. Kleij, *Adv. Synth. Catal.* **2012**, *354*, 469-476; c) J. Rintjema, W. Guo, E. Martin, E. C. Escudero-Adán, A.W. Kleij, *Chem. Eur. J.* **2015**, *21*, 10754-10762; d) D. J. Darensbourg, A. Horn, Jr., A. I. Moncada, *Green Chem.* **2010**, *12*, 1376-1379.
- [10] a) T. M. McGuire, E. M. López-Vidal, G. L. Gregory, A. Buchard, *J. CO<sub>2</sub> Util.* **2018**, *27*, 283-288; b) G. L. Gregory, M. Ulmann, A. Buchard, *RSC Adv.* **2015**, *5*, 39404-39408; c) M. Honda, M. Tamura, K. Nakao, K. Suzuki, Y. Nakagawa, K. Tomishige, *ACS Catal.* **2014**, *4*, 1893-1896; using halohydrins: d) T. Hirose, S. Shimizu, S. Qu, H. Shitara, K. Kodama, L. Wang, *RSC Adv.* **2016**, *6*, 69040-69044.
- [11] C. Qiao, A. Villar-Yanez, J. Sprachmann, B. Limburg, C. Bo, A: W. Kleij, *Angew. Chem. Int. Ed.* **2020**, *59*, 18446-18451.
- [12] a) M.-Y. Wang, Y. Cao, X. Liu, N. Wang, L.-N. He, S.-H. Lia, *Green Chem.* **2017**, *19*, 1240-1244; b) J.-H. Ye, L. Song, W.-J. Zhou, T. Ju, Z.-B. Yin, S.-S. Yan, Z. Zhang, J. Li, D.-G. Yu, *Angew. Chem. Int. Ed.* **2016**, *55*, 10022-10026; c) Z.-B. Yin, J.-H. Ye, W.-J. Zhou, Y.-H. Zhang, L. Ding, Y.-Y. Gui, S.-S. Yan, J. Li, D.-G. Yu, *Org. Lett.* **2018**, *20*, 190-193; d) L. Sun, J.-H. Ye, W.-J. Zhou, X. Zeng, D.-G. Yu, *Org. Lett.* **2018**, *20*, 3049-3052. For a somewhat related strategy providing cyclic carbamates: c) J.-H. Ye, L. Zhu, S.-S. Yan, M. Miao, X.-C. Zhang, W.-J. Zhou, J. Li, Y. Lan, D.-G. Yu, *ACS. Catal.* **2017**, *7*, 8324-8330. For a related review on radical carboxylative cyclizations: d) J.-H. Ye, T. Ju, H. Huang, L.-L. Liao, D.-G. Yu, *Acc. Chem. Res.* **2021**, *54*, 2518-2531.
- [13] a) C. Zhang, *Org. Biomol. Chem.* **2014**, *12*, 6580-6589; b) H. Li, *Synlett.* **2012**, *23*, 2289-2290.
- [14] Note that we observed formation of small amounts (typically 5-10%) of hydrolyzed cyclic carbonate in several experiments, which explains the loss of some or more material upon purification. The 1,3-diol byproducts have high  $R_f$  values and do not contaminate the final product.
- [15] The current hypothesis is that **2a** over a period of time is decomposed by the borosilicate glass of the vial in which it was kept.
- [16] M. Helou, O. Miserque, J.-M. Brusson, J.-F. Carpentier, S. M. Guillaume, *Chem. Eur. J.* **2010**, *16*, 13805-13813.
- [17] Y. Song, X. Yang, Y. Shen, M. Dong, Y.-N. Lin, M. B. Hall, K. L. Wooley, *J. Am. Chem. Soc.* **2020**, *142*, 16974-16981.
- [18] T. M. McGuire, C. Pérale, R. Castaing, G. Kociok-Köhn, A. Buchard, *J. Am. Chem. Soc.* **2019**, *141*, 13301-13305.
- [19] O. Phillips, J. M. Schwartz, P. A. Kohl, *Polym. Degrad. Stab.* **2016**, *125*, 129-139.
- [20] K. J. Zhu, R. W. Hendren, K. Jensen, C. G. Pitt, *Macromolecules* **1991**, *24*, 1736-1740.
- [21] G. M. Sheldrick, SHELXTL Crystallographic System, version 6.10; Bruker AXS, Inc.: Madison, WI, **2000**.

Photocatalytic Synthesis of Novel Cyclic Carbonate Monomers for Ring-Opening Polymerization

*Adv. Synth. Catal.* **2021**, *363*, Page – Page

Cristina Maquilón, Francesco Della Monica, Bart Limburg\* and Arjan W. Kleij\*

